Supplementary data for:

PROBING THE LOCAL ELECTRONIC AND GEOMETRIC PROPERTIES OF THE HEME IRON CENTER IN A HEME-NITRIC OXIDE AND/OR OXYGEN BINDING DOMAIN

Zhou Dai and Elizabeth M. Boon

From Department of Chemistry, Stony Brook University, Stony Brook, NY 11794-3400

Address correspondence to: Elizabeth M. Boon, Department of Chemistry, Stony Brook University, Stony Brook, NY 11794-3400, USA.

Telephone: +1 631 632 7945. Email: elizabeth.boon@stonybrook.edu

Table of Contents

Supplemental introduction to *Tt* H-NOX heme distortion.

Tt H-NOX WT crystallized in two different crystal forms, orthorhombic and monoclinic, with two molecules per asymmetric unit in both crystal forms, yielding four independent views of the protein [1]. Three of the four structures have severely distorted heme groups with approximately -1 Å saddling and -1.2 Å ruffling. The fourth molecule, however, has only approximately -0.7 Å displacement for both saddling and ruffling. *Tt* H-NOX P115A crystallized with four different molecules in the unit cell [2]. Two of the four structures have significantly flatter heme structure than wildtype, with approximately 0 Å saddling and -0.5 Å ruffling; the other two molecules are flatter than wildtype, but not dramatically so, with approximately -0.4 Å saddling and -0.6 Å ruffling each.

Electronic absorption and resonance Raman spectra measured for *Tt* H-NOX wildtype and P115A were used to determine the heme conformation in solution [2-4]. The electronic absorption spectra demonstrate a minimal perturbation caused by the mutation. However, peak broadening in several regions of the resonance Raman spectrum of the P115A mutant implies structural heterogeneity brought about by the heme relaxation within the porphyrin macrocycle. Furthermore, it was also found that there are dramatic changes in the reduction potential and ligand binding affinity upon the P115A mutation, as well as a shift in the conformation of the N-terminal region of the protein [2]. These results demonstrate that while H-NOX heme structure is dynamic, there is a clear link between heme conformation and *Tt* H-NOX structure, and that heme distortion is an important determinant for maintaining biochemical properties in H-NOX proteins.

Figure S1. XANES spectra of all 16 hemoprotein complexes.

Myoglobin samples: A. Mb Fe(II)-unligated; B. Mb Fe(II)-CO; C. Mb Fe(II)-O_2; and D. Mb Fe(III)-H_2O. *Tt* H-NOX samples: E. WT Fe(II) unligated; F. WT Fe(II)-CO; G. WT Fe(II)-NO; H. WT Fe(II)-O_2; I. WT Fe(III)-H_2O; J. WT Fe(III)-CN^-; K. P115A Fe(II) unligated; L. P115A Fe(II)-CO; M. P115A Fe(II)-NO; N. P115A Fe(II)-O_2; O. P115A Fe(III)-H_2O; and P. P115A Fe(III)-CN^-.

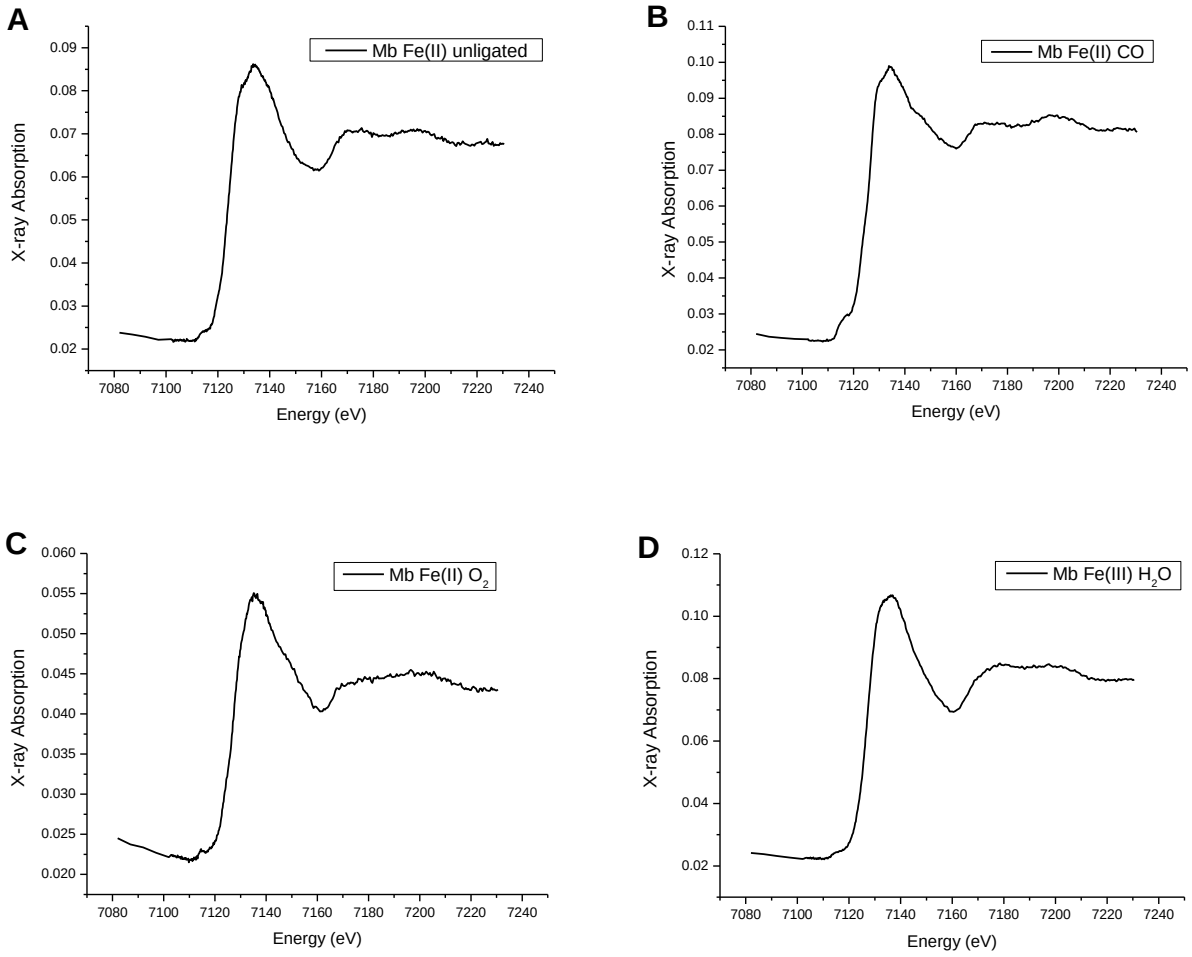

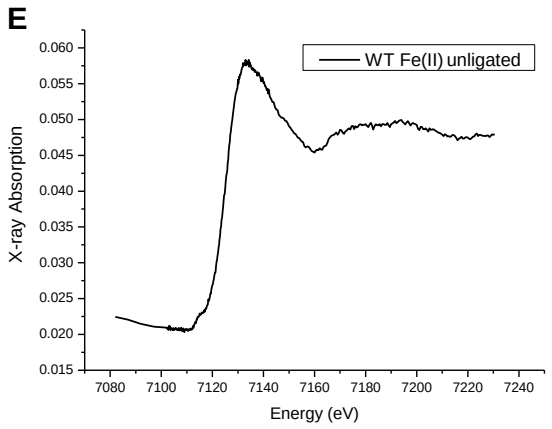
E
WT Fe(II) unligated
X-ray Absorption
Energy (eV)

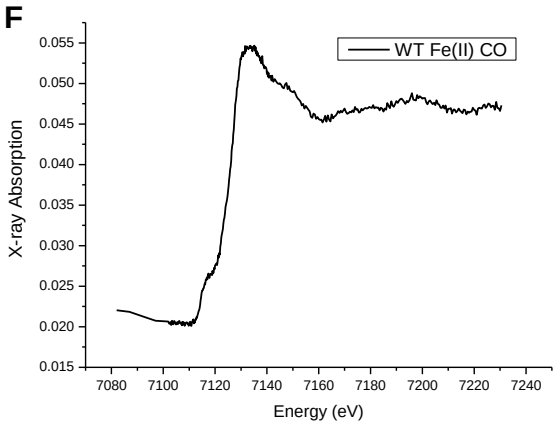
F
WT Fe(II) CO
X-ray Absorption
Energy (eV)

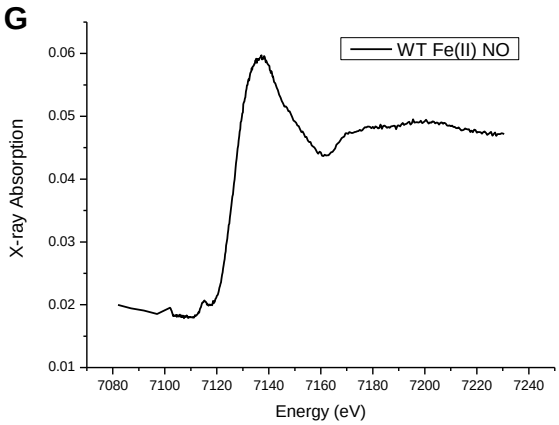
G
WT Fe(II) NO
X-ray Absorption
Energy (eV)

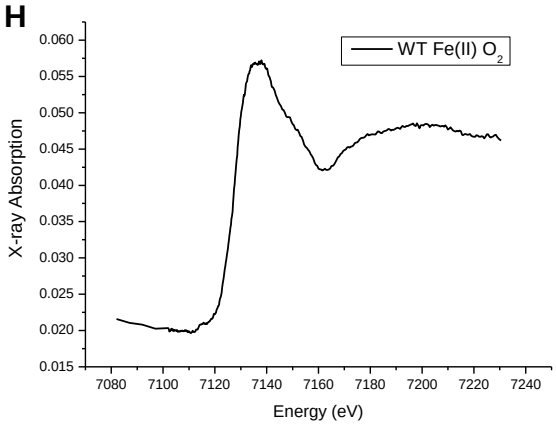
H
WT Fe(II) O2
X-ray Absorption
Energy (eV)

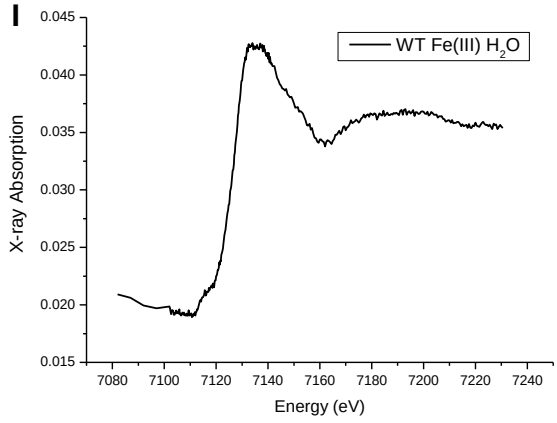
I
WT Fe(III) H2O
X-ray Absorption
Energy (eV)

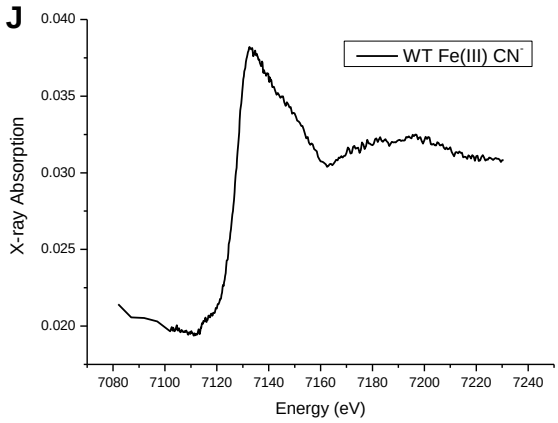
J
WT Fe(III) CN-
X-ray Absorption
Energy (eV)

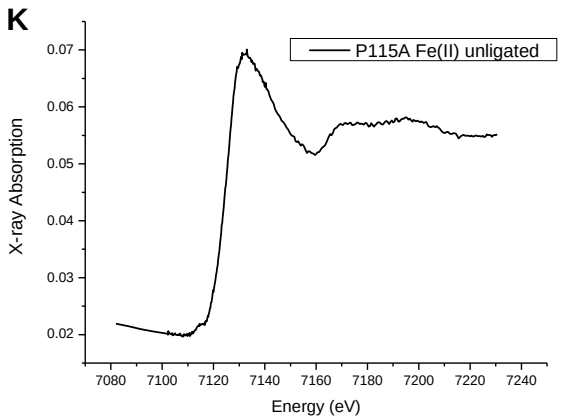
K
P115A Fe(II) unligated
X-ray Absorption
Energy (eV)

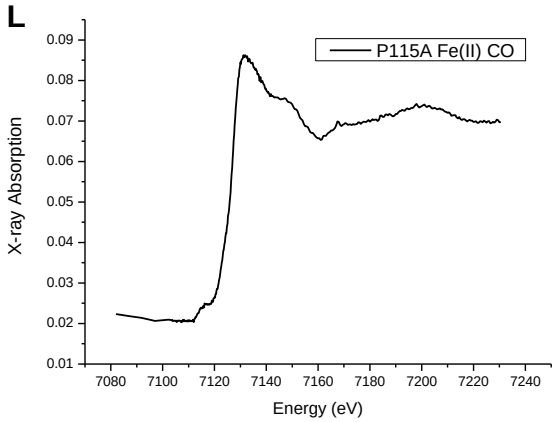
L
P115A Fe(II) CO
X-ray Absorption
Energy (eV)

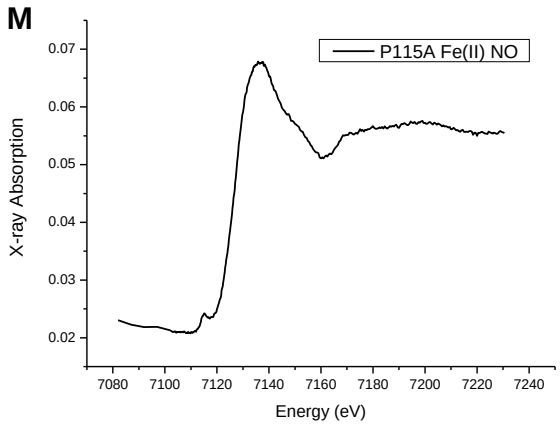
M
P115A Fe(II) NO
X-ray Absorption
Energy (eV)

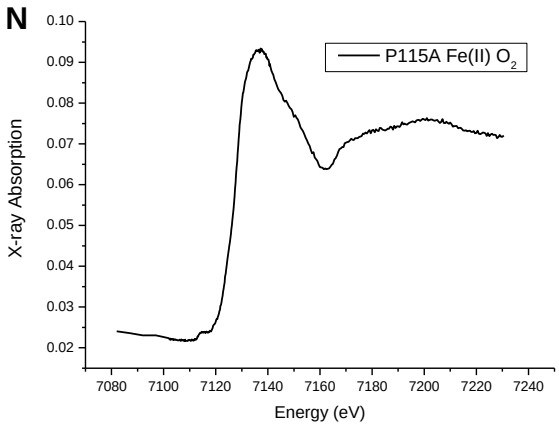
N
P115A Fe(II) O2
X-ray Absorption
Energy (eV)

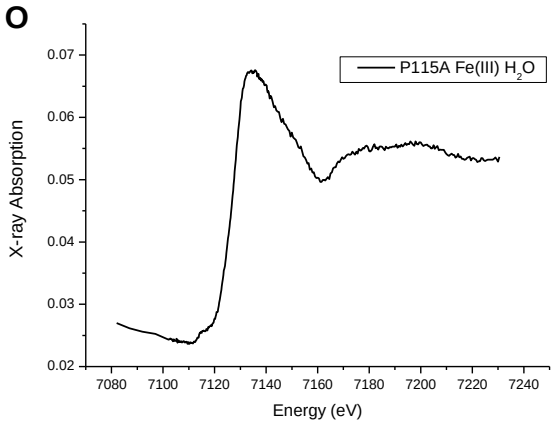
O
P115A Fe(III) H2O
X-ray Absorption
Energy (eV)

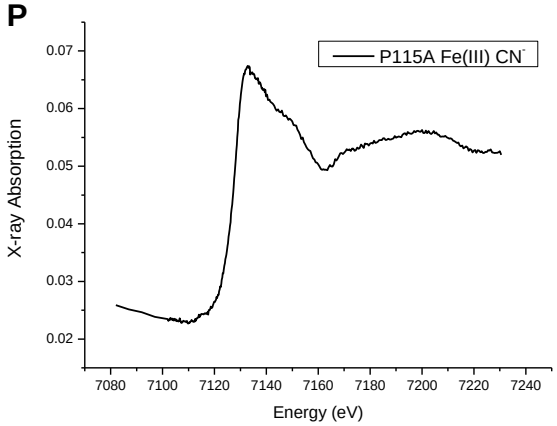
P
P115A Fe(III) CN-
X-ray Absorption
Energy (eV)

Supplemental discussion on LFIR and ligand binding affinities.

Fe-Ct displacement has been correlated with ligand binding affinity in Hb. For example, in the low affinity (T) form of hemoglobin, it has been shown that the iron is out of the heme plane by ~0.08 Å more than in the high affinity (R) form [5]. Considering that Fe-Ct displacement can be predicted from LFIR, ligand binding properties can also be predicted from the LFIR data. Here we make a more detailed discussion on the correlation between LFIR and ligand binding affinities.

We observed large differences in CN^- binding properties of WT versus P115A *Tt* H-NOX. We found that cyanide binds to WT Fe(III) (k_{on} = 26.9 s^{-1} M^{-1}) almost 2000 times faster than to P115A Fe(III) (k_{on} = 0.0153 s^{-1} M^{-1}), and values of K_D for WT and P115A Fe(III)-CN^- are determined to be 81.3 nM and 290 nM, respectively [6]. The rates of association and dissociation of CN^- in *Tt* H-NOX reflect the overall barrier of CN^- binding and leaving, respectively. The barriers mainly involve the diffusion of the ligand through the protein matrix and the interaction of the ligand with heme at the heme pocket. The ligand diffusion rates are expected to be similar for WT and P115A *Tt* H-NOX as they have the same protein fold. Thus, the differences in equilibrium and rate constants for CN^- binding to WT and P115A ferric heme are attributed to the interaction of CN^- with the heme pocket and can be understood using the LFIR prediction of Fe-Ct displacement.

As shown in Table 2 in the paper, during the replacement of water during CN^- binding to the ferric heme, the central iron in P115A *Tt* H-NOX experiences a much larger shift (0.16 Å) than that for WT (0.06 Å), which may subsequently lead to a larger shift of proximal histidine as well as the whole protein conformation based on our discussion. All these movements contribute to a larger activation energy for the P115A mutant.

Steric hindrance also plays an important role in ligand binding. In this case, the iron in the WT *Tt* H-NOX Fe(III)-CN^- complex is located almost exactly at the center of the porphyrin nitrogens, while the iron in the P115A *Tt* H-NOX Fe(III)-CN^- complex moves dramatically into the distal pocket where cyanide locates; we suggest that this results in a more crowded distal heme pocket, and hence larger steric

hindrance, consequently leading to a larger energy barrier for both CN^- association with and dissociation from P115A Fe(III). Thus k_{on} and k_{off} values for P115A are both much smaller than those measured for WT. Also due to the larger steric strain, the Fe(III)-CN^- complex for P115A is not as stable as that for WT *Tt* H-NOX, as indicated by the equilibrium dissociation constants.

Following this logic, we would also expect ferrous WT *Tt* H-NOX to have slightly greater affinity than its P115A analog for oxygen, due to its slightly smaller Fe-Ct displacement. However, it has been determined that the association and dissociation rate constants of O_2 binding to ferrous WT are 13.6 $s^{-1}\mu M^{-1}$ and 1.22 s^{-1} respectively, and to ferrous P115A are 10.4 $s^{-1}\mu M^{-1}$ and 0.22 s^{-1}, respectively [2]. These data indicate that oxygen binds to ferrous P115A more tightly than to ferrous WT *Tt* H-NOX. This disagreement is resolved upon consideration of the importance of H-bonds in stabilizing the H-NOX oxygen complex, however. It has been demonstrated that a strong H-bond between tyrosine 140 and bound oxygen is essential for oxygen binding in the H-NOX family [7]. Inspection of the Fe(II)-O_2 crystal structures indicates that, in P115A the Tyr-OH is ~0.3 Å closer to the bound oxygen molecule than in WT, which is reflective of the change in Fe-Ct displacement. This suggests a stronger H-bond and thus a larger oxygen stabilization effect for the *Tt* H-NOX P115A oxy-complex. This stronger H-bond is supported by lengthening of the O-O bond in the oxygen molecule from 1.30 Å in the WT complex to 1.40 Å in the P115A complex, and the shortening of the Fe-O (O_2) bond from 1.80 Å in the WT complex to 1.74 Å in the P115A complex [1, 2].

Furthermore, in comparison to the Fe(II)-O_2 binding properties, the differences between WT and P115A Fe(III)-CN^- binding properties are much more extreme, reflecting the much larger differences observed in the LFIRs and Fe-Cts for this complex. As discussed, the predicted Fe-Ct values for ferrous oxy-complexes of WT and P115A are similar, while the difference between WT and P115A for the Fe(III)-CN^- complex is 0.10 Å. That the LFIR data do not pick up on the difference in affinity for O_2 is an indication of the sensitivity of this technique for predicting ligand binding affinity. This level of sensitivity is suggested in the Hb example discussed above; the iron atom and the heme are less coplanar

by ~0.08 Å in the low affinity (T) form of hemoglobin than the high affinity (R) form. Therefore, a more dramatic difference between WT and P115A for Fe(III)-CN^- binding is predicted from XAS measurements, as we have observed.

Based on this argument, we expect differences in the CO and NO affinities to be similar in scale to the differences observed in the O_2 affinities, as the differences in Fe-Ct displacements for these ligands are small. Indeed, we find that the NO dissociation rate constants for *Tt* H-NOX WT and P115A are more similar, 0.042 min^{-1} and 0.026 min^{-1}, respectively (unpublished results).

References

[1] P. Pellicena, D.S. Karow, E.M. Boon, M.A. Marletta, J. Kuriyan, Proc. Natl. Acad. Sci. U.S.A. 101 (2004) 12854-12859.

[2] C. Olea, E.M. Boon, P. Pellicena, J. Kuriyan, M.A. Marletta, ACS Chem. Biol. 3 (2008) 703-710.

[3] D.S. Karow, D. Pan, R. Tran, P. Pellicena, A. Presley, R.A. Mathies, M.A. Marletta, Biochemistry 43 (2004) 10203-10211.

[4] R. Tran, E.M. Boon, M.A. Marletta, R.A. Mathies, Biochemistry (2009)

[5] M. Chance, L. Parkhurst, L. Powers, B. Chance, J. Biol. Chem. 261 (1986) 5689-5692.

[6] Z. Dai, E.M. Boon, J. Am. Chem. Soc. 132 (2010) 11496-11503.

[7] E.M. Boon, S.H. Huang, M.A. Marletta, Nat. Chem. Biol. 1 (2005) 53-59.

Figure(s)

Click here to download Figure(s): DaiBoonFigureS1.pdf

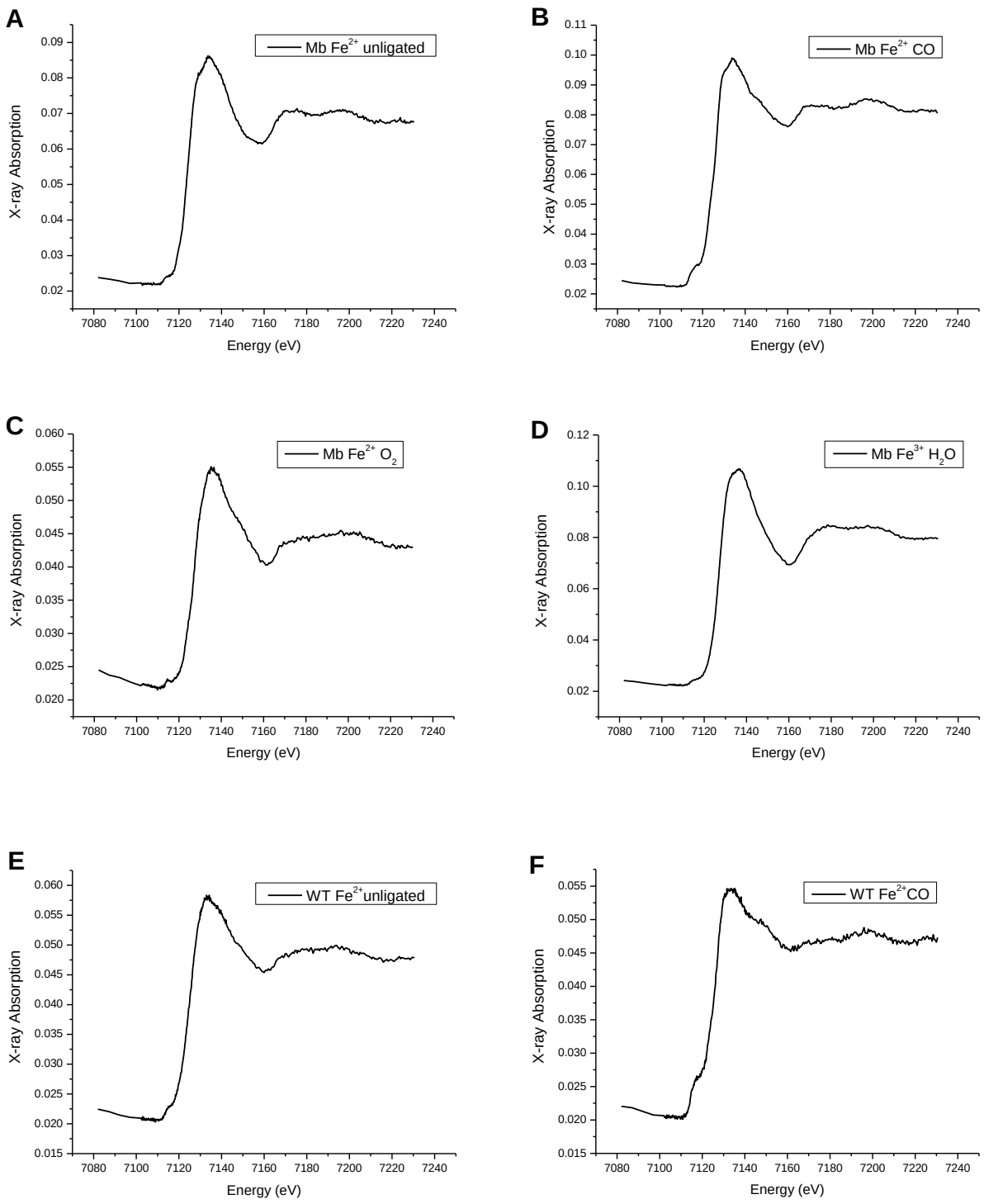

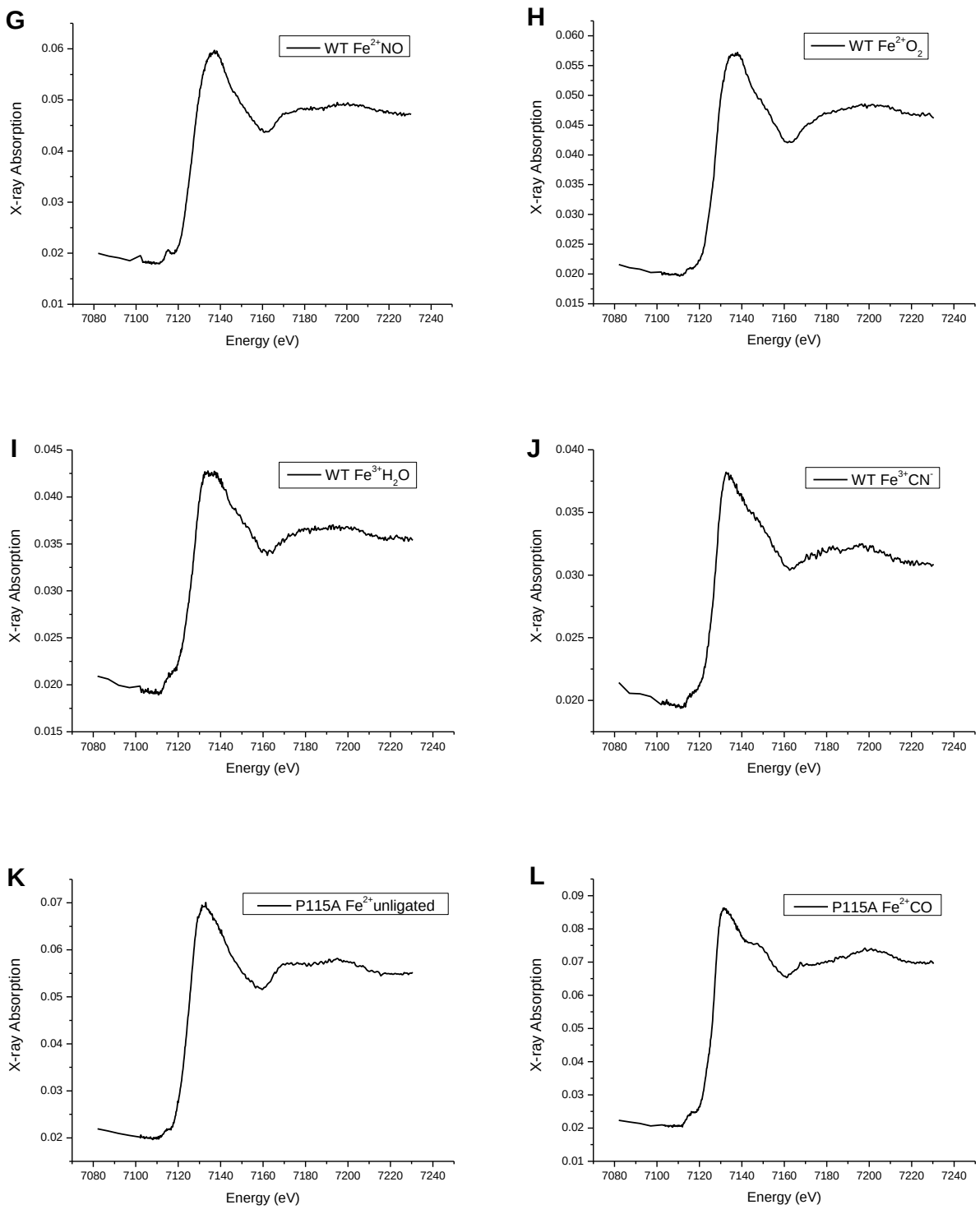
G
WT Fe2+NO
X-ray Absorption
Energy (eV)
H
WT Fe2+O2
X-ray Absorption
Energy (eV)
I
WT Fe3+H2O
X-ray Absorption
Energy (eV)
J
WT Fe3+CN-
X-ray Absorption
Energy (eV)
K
P115A Fe2+unligated
X-ray Absorption
Energy (eV)
L
P115A Fe2+CO
X-ray Absorption
Energy (eV)

M

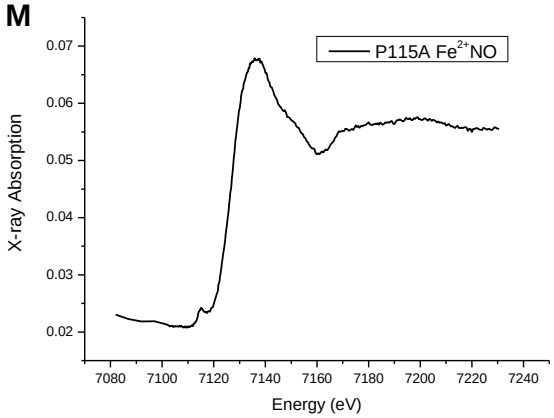
P115A Fe2+NO
X-ray Absorption
Energy (eV)
0.02
0.03
0.04
0.05
0.06
0.07
7080
7100
7120
7140
7160
7180
7200
7220
7240

N

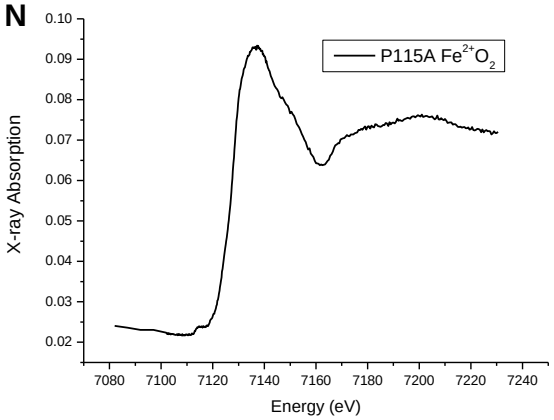
P115A Fe2+O2
X-ray Absorption
Energy (eV)
0.02
0.03
0.04
0.05
0.06
0.07
0.08
0.09
0.10
7080
7100
7120
7140
7160
7180
7200
7220
7240

O

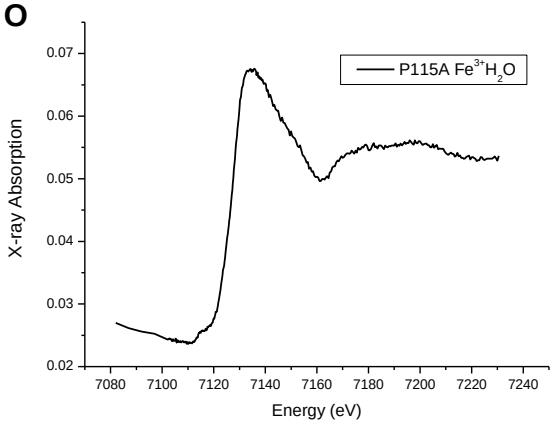
P115A Fe3+H2O
X-ray Absorption
Energy (eV)
0.02
0.03
0.04
0.05
0.06
0.07
7080
7100
7120
7140
7160
7180
7200
7220
7240

P

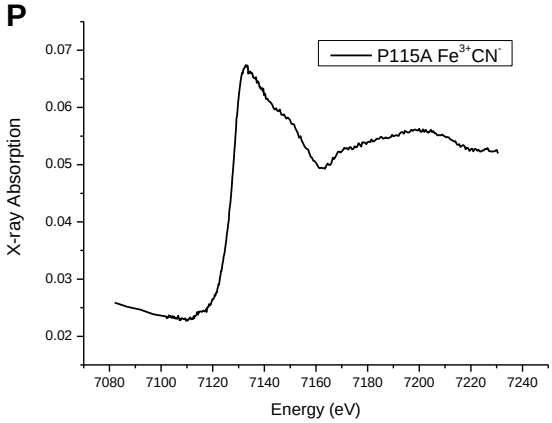
P115A Fe3+CN-
X-ray Absorption
Energy (eV)
0.02
0.03
0.04
0.05
0.06
0.07
7080
7100
7120
7140
7160
7180
7200
7220
7240